

## Simultaneous physisorption and chemisorption of reactive Orange 16 onto hemp stalks activated carbon: proof from isotherm modeling

Saeed Rehman<sup>1</sup>, Madiha Tariq<sup>1</sup>, Jehanzeb Ali Shah<sup>1</sup>, Rafiq Ahmad<sup>1</sup>, Muhammad Shahzad<sup>1</sup>, Arshad Mehmood Abbasi<sup>1</sup>, Aziz Ullah<sup>3</sup>, Bushra Ismail<sup>2</sup>, Muhammad Bilal<sup>1,\*</sup>

<sup>1</sup>Department of Environmental Sciences, COMSATS Institute of Information Technology, University Road, Tobe Camp Postal Code 22060, KPK, Abbottabad, Pakistan

<sup>2</sup>Department of Chemistry, COMSATS Institute of Information Technology, University Road, Tobe Camp Postal Code 22060, KPK, Abbottabad, Pakistan

<sup>3</sup>Department of Management Sciences, COMSATS Institute of Information Technology, University Road, Tobe Camp Postal Code 22060, KPK, Abbottabad, Pakistan

\*corresponding author e-mail address: [mbilal@ciit.net.pk](mailto:mbilal@ciit.net.pk)

### ABSTRACT

Innovative hemp stalk physically activated carbon (HSPAC) was used for reactive orange 16 (RO-16) dye fixation in aqueous solution. The HSPAC was characterized by Energy Dispersive X-ray Spectrometer (EDX) and Scanning Electron Microscopy (SEM). The performance of HSPAC was rated through adsorption of Reactive Orange 16 (RO-16) with respect to contact time, dose, particle size, initial dye conc., temperature and pH. Highest HSPAC adsorption capacity was found to be 32.21 mg/g with HSPAC dosage of 1 g/L at solution pH. The HSPAC surface reflected unique dual behavior and well demonstrated by Langmuir ( $R^2 = 0.994$ ) and Dubinin Radushkevich ( $R^2 = 0.994$ ) isotherm model. Pseudo second order kinetics model was found to be in close agreement with the experimental data, which also endorsed the unique simultaneous suitability of physisorption and chemisorption mechanisms in isotherm models. Values of thermodynamics constants ( $\Delta G^\circ > 0$ ,  $\Delta S^\circ < 0$ , and  $\Delta H^\circ < 0$ ) confirmed the adsorption of RO-16 onto HSPAC as non-spontaneous and exothermic.

**Keywords:** *Hemp stalk, Kinetics, Physically Activated Carbon, Physisorption, Chemisorption, Reactive Orange 16.*

### 1. INTRODUCTION

A large number of hazardous dyes and pigments generated by textile industries are released into water reservoirs as wastewater [1]. The persistent nature of color creates complications in remediating such wastewaters, even after the conventional treatment process [2, 3]. It is more severe in case of dissolved acids and reactive dyes, which stay even after conventional treatment system. Moreover, most of dyes have mutagenic or carcinogenic effects, that cause serious health hazards [4]. Therefore, the efficient treatment techniques are necessary for the degradation and/or removal of dyes in wastewater. A number of treatment methods such as ozonation [5], oxidation [6], coagulation [7], fungal degradation [8], and adsorption [9] have been proposed for dye removal from waste effluents. Among these methods, adsorption technique got reputation as efficient removal technology for dyes treatment due to simplicity in operation, cost effectiveness and low levels of sludge production. However, for practical applications the development of biomaterials for adsorption is a key. A number of adsorbents have been developed but activated carbon (AC) is preferred for dyes adsorption [10]. Therefore, AC has been extensively studied due to its high porosity [11], high surface area and large pore to volume ratio which are important factors for the efficient adsorption.

Due to such properties, dependency on activated carbon has got worldwide attraction. In 2012 the international demand for AC was around 4.2 million metric tons, which was anticipated to be

maintained at 10% per annum increment. The elevated demand of ACs is due to the reason of forceful pollution controlling strategies in China and America, as for example, in China (2011-2015), the twelfth five years plan, pursues the air and water quality to improve through utilizing environmental friendly techniques, which will likely increase the ACs demand.

Practically, the porosity in AC development is determined by the composition of plant materials containing cellulose, hemicelluloses, and lignin [12]. Such plant materials contain special functional groups (carboxyl, alcohols, ketones, aldehydes, and ether), which adhere to the dyes molecules in aqueous solution to make complexes [13]. In AC preparation a variety of organic precursor feedstock are used due to their high carbon contents [14].

For purity enhancement of carbon contents, the development of AC needs two popular methods namely, chemical activation and physical activation [15]. Physical activation is gaining much interest in industrial research as it allows numerous advantages as compared to so called chemical activation as for instance, high pyrolysis temperature, extensive use of chemicals acids, bases and different salts etc are major reasons. On the other hand, physical activation needs comparatively low temperature of activation, with no demand of chemicals.

Presently, an increasing trend in research on AC production derived from cheaper agriculture precursors is noticed. Being renewable, agriculture wastes are precious precursors for AC

production due to economically viable access. Therefore, the abundant availability makes agriculture waste a sustainable choice. This way the cost of waste disposal will also be reduced with sustainable production of AC [16]. Previously, massive research on AC production from agri-waste biomass has been conducted such as buriti shells [17], curcas pods [18], grape industrial waste [19] and tomato industrial waste [20].

Hemp is also important agriculture waste in Pakistan, which is cultivated on 840 hectares area producing > 500 tons of plant per annum [21]. To the best of our knowledge, no study is conducted on hemp stalk (*Cannabis sativa*) for production of physically AC. In this study, our objective is to investigate hemp stalk biomass as novel precursor for the lab scale production of hemp stalk physically activated carbon (HSPAC). This HSPAC will be used for adsorption of non-biodegradable, anionic

## 2. EXPERIMENTAL SECTION

**2.1. Adsorbate Preparation.** Analytical grade anionic RO-16 ( $C_{20}H_{17}N_3Na_2O_{11}S_3$ , molecular weight 617.52 g/mol) was chosen for adsorption studies on lab scale HSPAC. The UV/Vis spectra of RO-16 reflected a peak at 493 nm. The dye stock solution (1000 mg/L) was obtained by 1g dissolution of RO-16 powder in 1 liter of lab scale deionized water. Desired concentrations of dye were obtained by precise diluting of stock solution in definite proportion. Before and after adsorption monitoring of the solution concentration was conducted using double beam UV/Vis spectrophotometer (T80+ PG instrument, UK). The known concentration of RO-16 was used as calibration curve.

**2.2. Preparation of Hemp Stalk Physically Activated.** The hemp stalks used in present study were collected from the surrounding of Abbottabad. It was water flushed, cleaned and cut into tiny pieces and kept at 80 °C over-night in oven for moisture removal. Then it was put to one hour carbonization in muffle furnace (KLS 30/11, ThermConcept, Germany) at 160 °C in N<sub>2</sub> stream. After that physical activation of the hemp stalk was conducted in CO<sub>2</sub> stream. In the activation process the interaction of carbon (HSPAC) was allowed with CO<sub>2</sub> at 300 °C, which facilitates the production of high surface area porous structures that have molecular characteristics. After the activation process samples were let to cool down at natural pace in CO<sub>2</sub> stream. The carbon produced was taken for the dye treatment through batch (WiseCube Orbital Shaker) method. Since this method did not produce chemical wastes, needed low energy input, it is more eco-friendly as compare to conventional chemical activation.

**Table 1.** Experimental parameters with respective range for RO-16 adsorption onto HSPAC.

Contact time	Initial conc.	Ads. Dose	Particle size	pH	Temperature
0 - 480 min	30 – 300 mg/L	0.3 – 5 gL <sup>-1</sup>	125-840 μm	2-11	25-50 °C

**2.5. Isotherms, Kinetics and Thermodynamics Studies.** The obtained equilibrium data has been put to analysis, in light of three isotherm models namely Langmuir, Freundlich and Dubinin Radushkevich (D-R). The method of kinetics studies was analogous to that applied for equilibrium adsorption studies. However, the kinetics studies were conducted at four concentrations (30 mg/L, 50 mg/L, 75 mg/L and 100 mg/L). The

sulfonated reactive [22] azo dye, reactive orange 16 (RO-16). For this aim, carbonization (160 °C) and activation (300 °C) of hemp stalk were conducted in order to produce our desired HSPAC for improved dye uptake from aqueous solution. Consequent physico-chemical characteristics of HSPAC were identified under standard optimum conditions of special technologies such as scanning electron microscopy (SEM), and energy dispersive x-ray (EDX). Further, the lab scale HSPAC was used for removal of RO-16 dye from model aqueous solution as function of pH, contact time, sorbent dose, adsorbate concentration, particle size and temperature. The rate and mechanism of the reaction was also assessed through kinetics and isotherm studies. Thermodynamic analyses were also conducted to study thermal behavior of lab scale HSPAC.

**2.3. Morphology and Elemental Analysis of HSPAC.** The morphology of HSPAC before and after adsorption of RO-16 was studied by scanning electron microscopy (Hitachi Japan, S-3000N). The determination of standard elemental analysis was conducted by energy dispersive X-ray (EDX) method.

**2.4. Batch Experiments.** The experimental parameters with respective range are summarized in Table 1. The performance determination of HSPAC for RO-16 removal from model solution was determined through batch method. The adsorption system was launched with 50 mL adsorbate solution in different borosilicate flasks. The fixed amount of adsorbent (50 mg) was put to each flask and shaking incubated for 140 min. After all, the samples were centrifuged at 3000 rpm and consequent supernatant was filtered. The residual RO-16 concentration was measured using UV/Vis spectrophotometer (T80+ PG instrument, UK) at λ<sub>max</sub> of 494 nm. The adsorption of RO-16 at equilibrium was measured by q<sub>e</sub> (mg/g) as follow:

$$q_e = \frac{C_o - C_f}{m} V$$

Where V implies on solution volume (L), C<sub>e</sub> and C<sub>o</sub> shows initial and final concentration (mg/L), and m indicates adsorbent mass (g).

The removal percent (% R) of RO-16 was measured by following equation:

$$S(\%) = \frac{C_i - C_f}{C_i} \times 100$$

kinetics studies provide important information about RO-16 removal process as a time function. The pre-planned withdrawn of samples at specific time intervals from reaction flasks were conducted and the residual RO-16 concentrations were measured. The thermodynamic parameters ΔG (free energy change; kJ/mol), ΔH (enthalpy change; kJ/mol), and ΔS (chaos change; kJ/mol) were also studied to understand the behavior of adsorption.

### 3. RESULTS SECTION

**3.1 SEM and EDX Analysis.** Figure 1 shows SEM micrographs of different magnification of HSPAC surface before (a) and after (b) RO-16 uptake. The physically activated smooth surface of HSPAC (Fig. 1a) is due to elimination of impurities (hemicelluloses and lignin etc.) after carbonization and activation. The efficient adsorption of RO-16 is witnessed by uniform pore distribution of HSPAC, which facilitates dye adsorption even in secondary and tertiary pores [23, 24]. EDX demonstrated (Fig.1)

the quantitative presence of different elements by weight in HSPAC. The HSPAC was mainly composed of C (64.46%), O (34.42%), K (0.87%) and Ca (0.25%) before RO-16 uptake. The presence of RO-16 onto HSPAC was confirmed by elemental composition change after RO-16 treatment. The sample constituted C (63.44%), O (32.83%), and S (1.12%). The presence of C, S and O verified the dye uptake by HSPAC.

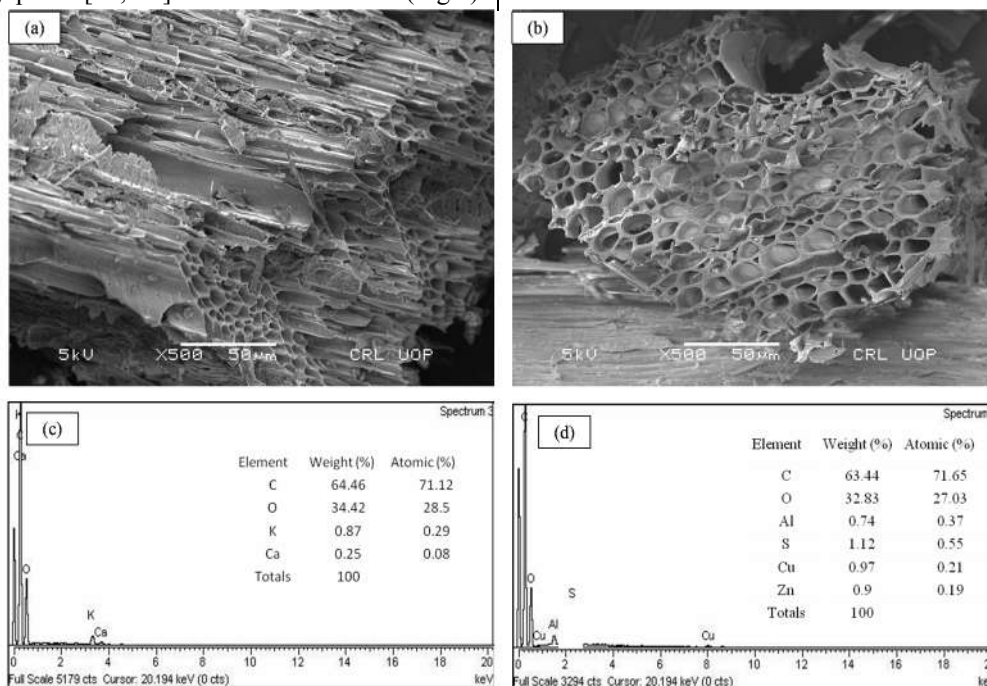


Figure 1. SEM micrographs (a) AC before, (b) AC after RO-16 adsorption; EDX spectra (a) AC before, (b) AC after RO adsorption.

**3.2. Equilibrium Time.** Adsorption on hemp stalk physically activated carbon (HSPAC) was studied as function of contact time in order to analyze the equilibrium time. The concentration influence on RO-16 adsorption was explored to determine the removal capacity. Figure 2 shows the adsorption capacity of RO-16 at initial dye concentration 50 mg/L and 0.05 g adsorbent dose (50 mL)<sup>-1</sup> solution and natural solution pH. The removal capacity rose with raise in contact time and reaches up to maximum 14.8 mg/g (29.59%) in 240 min. After that there were no further RO-16 uptake and a straight line is achieved.

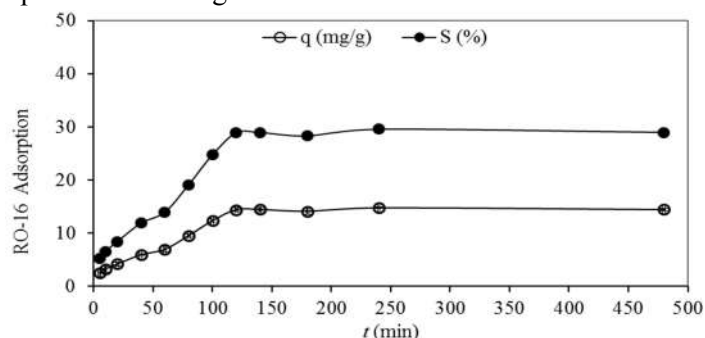


Figure 2. Effect of contact time on HSPAC-RO-16 adsorption system.

The fast adsorption of anionic RO-16 in the beginning is subjected to the availability of vacant charged sites on cationic adsorbent surface, which supported rapid adsorption of anionic RO-16 from aqueous solution. At elevated time, electrostatic repulsion could persist between the RO-16 and HSPAC surface due to the presence of positive charged species (H<sup>+</sup>) at low pH. Further, due to gradual pore diffusion of RO-16 into the aggregated adsorbent particles the adsorption rate does not alter significantly (p = 0.01) after 240 min. Therefore, this point was considered optimum for subsequent work on 50 mg/L of RO-16 adsorption. Similar results were also found in some previous literature [23].

**3.3. Adsorbent Dose.** The amount of HSPAC for given initial dye concentration determines the removal capacity of adsorbent. The amount effect of HSPAC onto RO-16 removal is depicted in Figure 3. At first, the adsorption efficiency increased (22.7 – 38.6%) swiftly with increase in HSPAC amount. After 2 g of HSPAC per liter of RO-16 solution, the removal capacity reached a uniform value.

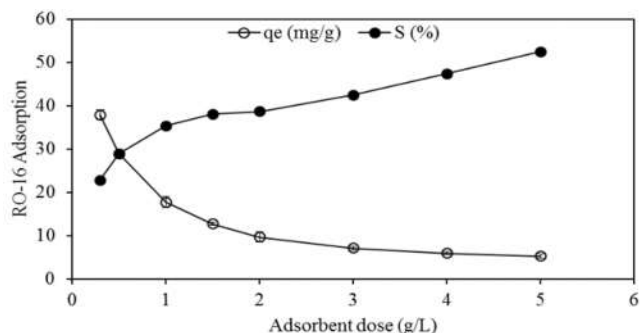


Figure 3. Adsorbent dose effect on HSPAC-RO-16 adsorption system.

Subsequently, the RO-16 removal efficiency increased from (38.6 – 52.5%) with increasing HSPAC dose (2 – 5 g/L) and decreasing removal capacity (9.65 – 5.25 mg/g). The increase in removal efficiency of dye could be due to availability of ample sorption vacant sites on adsorbent. These vacant sites are easily reachable for accommodation of less number of dye molecules in bulk of adsorbent. When the sorbent dose increased (1 – 5 g/L), significant high ( $p = 0.01$ ) removal efficiency of HSPAC was observed for RO-16 adsorption. Similar adsorbent dose findings were also found by previous studies [25].

**3.4. Particle Size.** The effect of particle size (125 – 840  $\mu\text{m}$ ) on HSPAC of RO-16 was investigated and the removal capacity and efficiency is shown in Figure 4. The significant high ( $p = 0.01$ ) increase is noticed in removal capacity of RO-16 (8.2 -19.83 mg/g) with decrease in particle size. This phenomenon could be attributed to total surface area of adsorbent, bared to dye molecules, which could facilitate the access of these molecules even through primary and secondary pores. Consequently, high number of binding sites could be accessible to dye molecules in smaller sized particles.

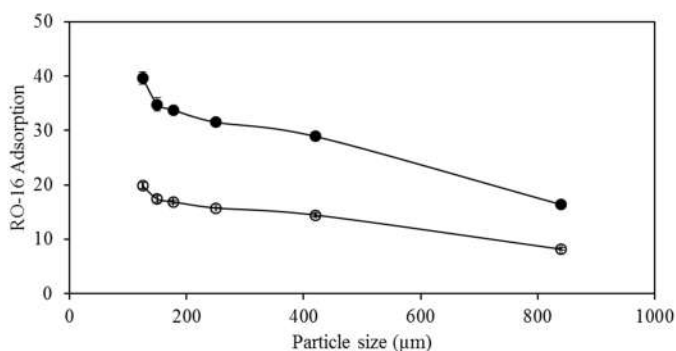


Figure 4. Particle size effect on HSPAC-RO-16 adsorption system.

**3.5. Initial Dye Concentration.** The concentration (25 -300 mg/L) effect of RO-16 onto adsorption of HSPAC was analyzed and the removal capacity and percentage was portrayed in Figure 5.

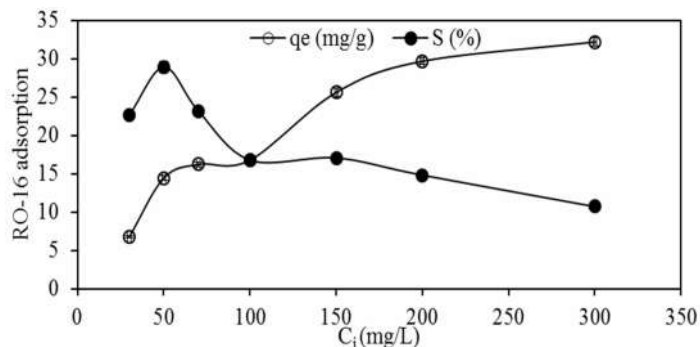


Figure 5. Initial dye concentration effect on HSPAC-RO-16 adsorption system.

The removal capacity of RO-16 increased from 6.81 mg/g to 17.09 mg/g with increase in dye concentration from 25 mg/L to 150 mg/L.

After 150 mg/L concentration of RO-16, the removal capacity decreases up to 10.74 mg/g. This is because, at low RO-16/HSPAC ratios, adsorption of RO-16 hold excited energy sites. As the RO-16/HSPAC ratio increases the energy sites saturates and the adsorption system begins on ground energy sites. Therefore, the removal efficiency decreases [26, 27].

**3.6. Effect of pH.** The solution pH is basic parameter governing the adsorption process for close linkage with surface charges of adsorbent and the rate of ionization energy of dye molecules [28]. In this work, the adsorption of RO-16 onto HSPAC is analyzed under varying pH (2 -11) and the findings are shown in Figure 6.

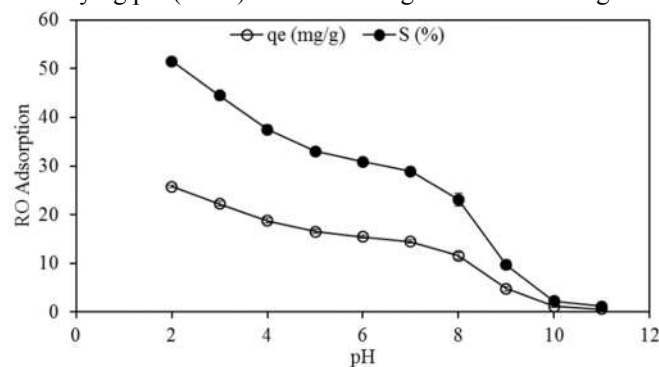


Figure 6. pH effect on HSPAC-RO-16 adsorption system.

The significant ( $p = 0.01$ ) high removal capacity (0.59 – 25.73 mg/g) was subjected with consistently lowering in pH from 11 to 2. The highest adsorption efficiency was found to be 51.4% at pH 2. Similar findings were previously reported by other scientists [29] and stated that strong ionic characters are responsible for such phenomenon under acid environment. Further, in acid environment, more protons are available, which exert repulsion on anionic RO-16 towards cationic HSPAC, as result the adsorption increases.

**3.7. Effect of Temperature.** Effect of varying temperatures (30 – 50  $^{\circ}\text{C}$ ) on removal efficiency and capacity of HSPAC-RO-16 system was studied using 50 mg/L of RO-16 at solution pH. Fig. 7 depicts that RO-16 removal capacity rises significantly ( $p = 0.01$ ) within the temperature rise from 5.21 mg/g to 14.46 mg/g. This phenomenon could be attributed to the fast diffusion of RO-16 ion (due to kinetic energy) from surrounding solution into the primary secondary and tertiary pores of HSPAC as confirmed by (Figure 7). These findings are compatible with the findings of some previous authors (Wu et al., 2016).

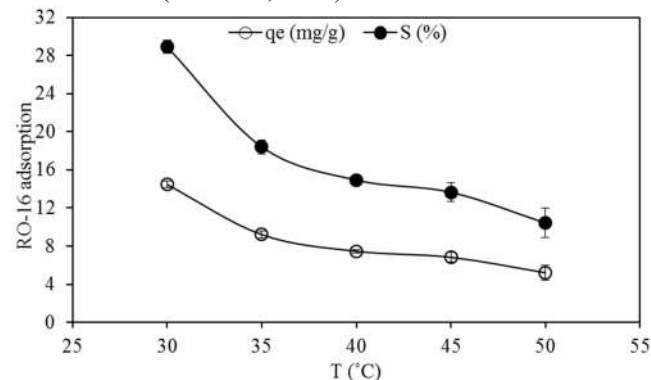
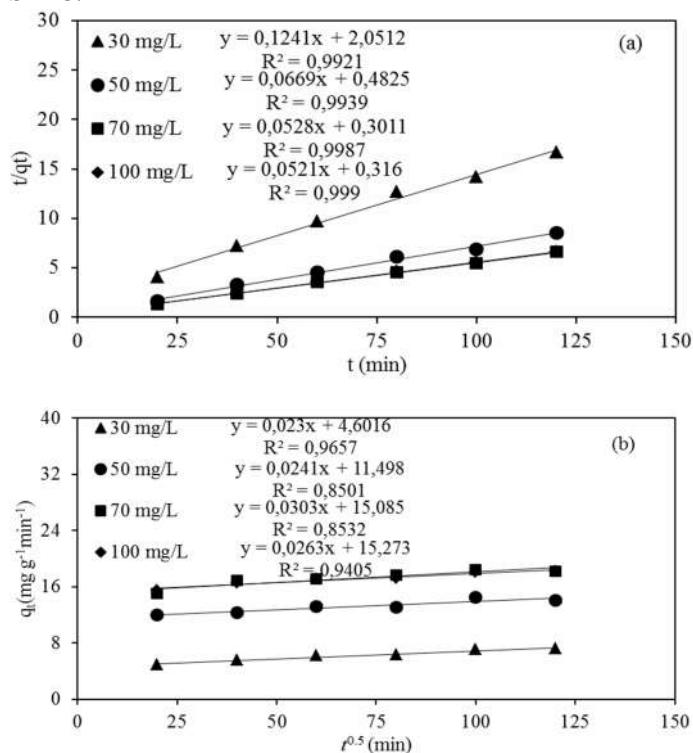


Figure 7. Temperature effect on HSPAC-RO-16 adsorption system.

**3.8. Kinetics Studies.** Adsorption kinetics analysis is important due to provision of worthy information on the rate and mechanism of reaction in adsorption system [30]. In order to study the adsorption kinetics of HSPAC, three models were applied namely pseudo-first order, pseudo second order and intra particle diffusion as shown in their respective linear plots (Fig 8). As mentioned in Table 2, that the initial concentration of RO-16 was 30 mg/L, 50 mg/L, 75 mg/L and 100 mg/L. HSPAC has high removal capacity, which practically adsorbed 41.79 mg/g (83.58%) of RO-16 from 50 mg/L solution.

The correlation of coefficients ( $R^2 = 0.99$ ) for initial four concentration levels confirmed the applicability of pseudo second order model (Table 2). As the constant ( $k_2$ ) is showing upward trend with increasing concentration (30 – 75 mg/L), which supports that the chemisorption is the step of determination in adsorption system. After 75 mg/L the  $K_2$  upward trend inverted, confirming that the chemisorption is not the only rate limiting factor. Therefore, both physisorption and chemisorption control the adsorption system at high concentrations (100 mg/L) of RO-16. Similar adsorption kinetic model was also fit best on the experimental data of Cu(II) and Cd(II) adsorption onto chitosan [31]. The intra particle diffusion model is responsive to diffusion mechanism of adsorbate in aqueous solution. The correlation of coefficients ( $R^2 = 0.965$ ;  $R^2 = 0.940$ ) for two concentration levels support the intraparticle diffusion best fit (Table 2) after pseudo second order model. The plot curve of this model (Figure 8) reflects two linear steps during adsorption process. In first step the RO-16 diffuses from adsorbate solution into the outer surface of HSPAC.

reflects two linear steps during adsorption process. In first step the RO-16 diffuses from adsorbate solution into the outer surface of HSPAC.



**Figure 8.** Pseudo-second order kinetic model (a) and intraparticle diffusion model (b) for HSPAC-RO-16 adsorption system.

**Table 2.** Kinetics models constants for HSPAC-RO16 adsorption system.

Adsorbent-Adsorbate	HSPAC - RO-16			
Pollutant Concentration (mg/L)	30	50	75	100
<b>Pseudo-first-order</b>				
$q_{e, exp}$ (mg/g)	7.21	14.46	18.23	18.21
$q_{e, cal}$ (mg/g)	3.95	3.64	4.92	4.23
$K_1$ (/mins)	0.0097	0.0092	0.0159	0.0111
$R^2$	0.953	0.0840	0.0918	0.0931
<b>Pseudo-second-order</b>				
$q_{e, exp}$ (mg/g)	24.7	41.79	58.77	85.98
$q_{e, cal}$ (mg/g)	8.05	14.14	18.93	19.19
$K_2$ (/mins)	0.0075	0.0092	0.0092	0.0085
$R^2$	0.992	0.993	0.998	0.999
<b>Intra-particle Diffusion</b>				
$Kp_i$ (mg/g min) <sup>1/2</sup>	0.023	0.0241	0.0303	0.0263
$C_i$ (mg/g)	4.60	11.49	15.8	15.27
$R^2$	0.965	0.850	0.853	0.940

In second step the intraparticle diffusion of RO-16 occurred from outer surface into the inner body of HSPAC adsorbent. Further, the value of  $C_i$  ( $0 <$ ) is consistently increasing, confirming the intraparticle diffusion is not the inhibiting step of the adsorption system. Thus, it is endorsed that the film and intraparticle diffusion, both is governing the adsorption system [32]. These findings are compatible with the results of previous authors [33].

**3.9. Isotherm Models.** Adsorption isotherm concerns with the linkage between adsorbate quantities uptaken by adsorbent with remaining concentration of adsorbate in solution. A number of isotherm equations have been used for experimental analysis of adsorption process. The parameters and constants used in these isotherm equations provide evidences of the adsorbent

compatibility with adsorbate, surface characteristics, and adsorption mechanism. The adsorption mechanism of this work is illustrated by Langmuir, Freundlich and D-R isotherm models. The experiments for isotherm model description (Table 3) of RO-16 were conducted from 25 to 30 °C, adopting standard conditions of experiments as described previously.

Langmuir explained the Langmuir isotherm [34], which reflects monolayer attachment mechanism on homogenous adsorbent surface. Following linear equation is used for this isotherm model.

$$\frac{C_e}{q_e} = \frac{1}{KLq_{max}} + \frac{C_e}{q_{max}}$$

Where  $q_e$  is removal capacity at equilibrium,  $C_e$  is adsorbate concentration at equilibrium,  $q_{max}$  is highest removal

capacity, and  $K_L$  is the equation constant, which is related to energy of adsorption.

Contrarily, Freundlich suggested the Freundlich isotherm model [35], which describes the Van der Waals attachment of solute concentration over surface of non-uniform adsorbent. Subsequent equation can be used to express the Freundlich calculations.

$$q_e = K_F C_e^{1/n}$$

Where  $K_F$  and  $1/n$  are Freundlich coefficient and exponential coefficient (heterogeneity factor) respectively, which shows corresponding removal capacity and removal intensity in adsorption system. The  $K_F$  and  $1/n$  values are calculated by plot  $q_e$  vs  $C_e$ .

Dubinin-Radushkevich (D-R) is widely accepted equation, which proposed that mostly pore-filling mechanism is observed through Van der Waal attachment in adsorption system instead of covering around adsorbent in layers [36]. This approach is frequently adopted to discriminate the physisorption phenomenon from chemisorption. The equation of this model is as follow:

$$\ln = \ln q_{DR} - \beta \epsilon^2$$

Where  $q_{DR}$  (mg/g) denotes removal capacity,  $\beta$  (kJ/mol)<sup>2</sup> implies adsorption energy constant and  $\epsilon$  shows potential of Polanyi, in this study it describes the quantitative adsorption of liquid adsorbate.

Further, for one molecule of adsorbate uptake  $E$  can be measured as follow:

$$E = \left[ \frac{1}{\sqrt{2B_{DR}}} \right]$$

$B_{DR}$  denotes constant of isotherm, same time the parameter  $\epsilon$  can be measured as

$$RT \ln = \left[ \frac{1}{C_e} \right]$$

Where  $R$  (8.314/mol/k) is universal gas constant,  $T$  is absolute temperature, and  $C_e$  is equilibrium adsorbate concentration (mg/L).

The D-R model is strongly linked to temperature of the adsorption system. At varying temperatures the experimental

adsorption data when plotted as logarithmic function of quantity adsorbed ( $\ln q_e$ ) versus  $\epsilon$  (potential of energy)<sup>2</sup>, total suitable data will be appeared at the same characteristic curve [37]. Here we discuss on values and constants of aforesaid isotherm models.

**3.9.1. Langmuir Isotherm Model.** The  $q$  (41.32 mg/g) calculated by the isotherm model was in close compliance with the  $q$  (32.21 mg/g) found experimentally (Table 4). The model followed the best value of regression of coefficient ( $R^2 = 0.994$ ), which confirmed that monolayer chemisorption mechanism dominates the adsorption system of HSPAC-RO-16. This confirms that a bond of chemical nature is acting, which electrostatically attracts RO-16 towards HSPAC surface in aqueous solution. Hence, the energy of activation corresponds to the sorption of RO-16 in chemical bond formation. The  $R_L$  (0.423 L/mg) value confirms the adsorption favorability of RO-16 onto HSPAC surface [23]. Similar model also best fit on adsorption of RO-16 onto chitosan [22].

**3.9.2. Freundlich Isotherm Model.** The linear isotherm plot for RO-16 adsorption is depicted in Figure 9. The  $R^2$  (0.969) value is much lower than rest of the models, confirming worst fitting of the equilibrium data for the HSPAC-RO-16 adsorption system. However, it could be considered for heterogeneity of the HSPAC surface. This endorsed the non-uniform composition of binding sites of HSPAC for multilayer attachment of RO-16. The calculated  $n$  ( $> 1$ ) value (Tab. 3) recommends the adsorption process favorable [38]. The very low  $K_F$  value favors the weak bond linkage (Van der Waals) between RO-16 and HSPAC during physisorption phenomenon. The measured  $1/n$  ( $< 1$ ) value (0.0675) suggests the adsorption favorable, which supports feasibility of HSPAC for RO-16 adsorption in aqueous solution.

**3.9.3. D-R Isotherm Model.** The linear plot (Figure 9) supports that the regression of co-efficient ( $R^2 = 0.994$ ) of RO-16 adsorption shows well fit to D-R model isotherm. The adsorption energy constant  $\beta$  was estimated as (0.008 mol/j). The mean free energy of RO-16 from infinite up to active adsorption site onto HSPAC surface was 7.832 kJ/mol (Table.3).

**Table 3.** Isotherm constants for HSPAC-RO-16 adsorption system.

Isotherms Model	Adsorbate, RO-16	Units of parameters
Langmuir		
$q_{exp}$	32.21	mg/g
$q_{cal}$	41.32	mg/g
$R_L$	0.423	L/mg
$R^2$	0.0994	
Freundlich		
$1/n$	0.675	
$N$	1.48	
$K_F$	0.857	L/g
$R^2$	0.969	
D-R		
$q_{DR}$	37.40	mg/g
$B$	0.008	(mol/j) <sup>2</sup>
$E$	7.832	kJ/mol
$R^2$	0.994	

Previously suggested, that adsorption system having  $E$  value ( $8 < 16$  kJ/mol) will have attachment through chemisorption

[39]. Hence, it could be deduced that D-R model suggests the attachment of RO-16 onto HSPAC as physisorption phenomenon

as also confirmed by Freundlich isotherm model ( $R^2 = 0.969$ ). The  $R^2$  value of HSPAC-RO-16 adsorption system for D-R isotherm (Table 3) is exactly the same as the  $R^2$  value of Langmuir isotherm model. It attests that the HSPAC surface is dual natured showing simultaneous chemisorption and physisorption behavior to RO-16 uptake. It confirms that some molecules of RO-16 are adhered through strong chemical bond and the remaining through weak Van der Waal forces. Therefore, there could also be the probability of multilayer adsorption of RO-16 onto HSPAC; as also confirmed by pseudo second order model kinetics, which previously verified that the chemisorption is not the rate limiting step as physisorption also governs the adsorption system.

These unique findings of isotherm models having corresponding high  $R^2$  values are in the following order: Langmuir = D-R > Freundlich (Table 3). However, Langmuir model ( $R^2 = 0.994$ ) has key role in the HSPAC-R)-16 adsorption system as confirmed by energy value ( $E = 7.832$  kJ/mol) of D-R isotherm.

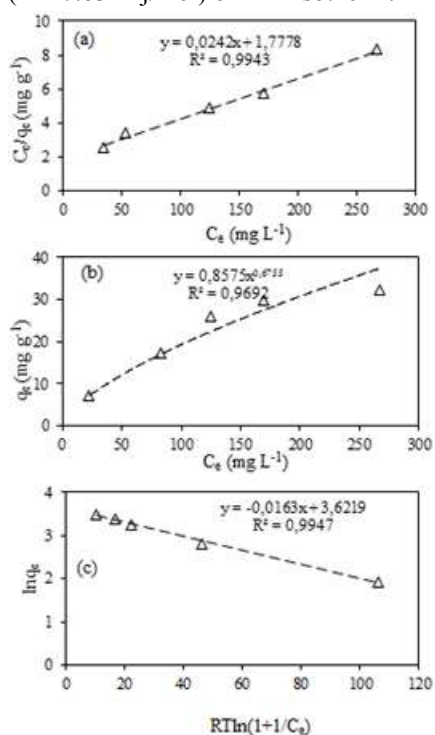


**Figure 9.** Isotherm fitness to HSPAC-RO-16 adsorption system: (a) Langmuir; (b) Freundlich; (c) D-R.

**Table 4.** Thermodynamic constants and parameters for HSPAC-RO-16 adsorption system.

$\Delta H$ (kJ mol <sup>-1</sup> )	$\Delta S$ (kJ mol <sup>-1</sup> )	$\Delta G$ (kJ mol <sup>-1</sup> )				
		303K	303K	313K	318K	323K
-60.79	-0.21	2.17	3.21	4.25	5.28	6.32

#### 4. CONCLUSIONS

In this study, the performance of HSPAC adsorbent was tested for RO-16 adsorption. The adsorption system (HSPAC-RO-16) was found to be strongly associated with contact time, dose, particle size, initial dye concentration, temperature and pH. The equilibrium time for HSPAC-RO-16 adsorption system was found to be 140 min. Dramatic increase in RO-16 uptake was noticed at pH 2, which gradually decreased with rise in pH. Highest adsorption capacity ( $q_m$ ) was found to be 37.92 mg/g. Isotherm studies reflected the unique fitness of the experimental data on

**3.10. Thermodynamic Analysis.** The thermodynamic parameters (Table 4) were specified to perceive the nature of HSPAC-RO-16 adsorption system. Determination of equilibrium constants of thermodynamics, change in free energy, and chaos change were undertaken for assessment of viability of thermodynamics and spontaneity of the system. The calculation of thermodynamic constants was conducted with the following equation:

$$\Delta G^\circ = -RT \ln K_e$$

Where  $\Delta G^\circ$  shows (free energy change in kJ/mol) R denotes (universal gas constant = 8.314 j/mol/k),  $K_e$  indicates (thermodynamic equilibrium constants) and T reflects (absolute temperature in K). Under different thermal conditions the constant ( $K_e$ ) is calculated from plot ( $\ln q_e/C_e$  Vs  $q_e$ ).

As witnessed by Table 4 that the non-spontaneous nature of the adsorption process was confirmed by positive  $\Delta G^\circ$ . Gradual increase of  $\Delta G^\circ$  value from 303 k to 323 k supports the dominant chemical bonding as also confirmed by Langmuir model in the adsorption system. Other parameters ( $\Delta H^\circ$  and  $\Delta S^\circ$ ) can be quantified from plot of Van't Hoff equation ( $\ln K^\circ$  Vs  $1/T$ ) as following:

$$\ln K^\circ = \frac{\Delta S^\circ}{R} - \frac{\Delta H^\circ}{RT}$$

As summarized in Table 4 the negative  $\Delta H^\circ$  value confirms the exothermic in the HSPAC-RO-16 system. The negative  $\Delta S^\circ$  reflects the decrease in RO-16 concentration in liquid solid interface. In the liquid solid interface of the present scenario, the adsorption process is integrated by two steps: (a) stripping out of previously adsorbed solvent molecules (RO-16) at elevated temperatures, (b) the adsorption of RO-16 onto HSPAC. The RO-16 molecules have to move several molecules/revolution to their respective binding sites onto HSPAC surface, which results in exothermic adsorption of dye [40]. Hence it proves RO-16 concentration decreased onto HSPAC surface in result of pore stripping mechanism (due to high temperature), which is also supported by physical bonding of D-R and Freundlich isotherm models. The negative ( $\Delta H^\circ$ ) may reflect, increase desorption of RO-16 that may lead to decrease adsorption capacity at high temperatures. Similar finding analogies could also be found elsewhere in adsorption of Reactive orange 12 and direct yellow 12 onto activated carbon [41, 42].

Langmuir and D-R models to confirm the dual behavior of HSPAC for RO-16 adsorption. This behavior was confirmed by pseudo second order model kinetics in which only chemisorption was not rate inhibiting step, i.e. it was physisorption as well. The process in adsorption system was found to be exothermic and non-spontaneous with negative chaos value. Hence, it is confidently concluded that the HSPAC could be used as competent adsorbent for RO-16 removal from aqueous solutions.

## 5. REFERENCES

- [1] Ghaedi M., Hajati S., Karimi F., Barazesh B., Ghezlbash G., Equilibrium, kinetic and isotherm of some metal ion biosorption. *Journal of Industrial and Engineering Chemistry*, 19, 987-92, **2013**.
- [2] Visa M., Bogatu C., Duta A., Simultaneous adsorption of dyes and heavy metals from multicomponent solutions using fly ash. *Applied Surface Science*, 256, 5486-91, **2010**.
- [3] Ravi Kumar M., Rajakala Sridhari T., Durga Bhavani K., Dutta P.K., Trends in color removal from textile mill effluents. *Colourage*, 45, **1998**.
- [4] Hejazifar M., Azizian S., Adsorption of cationic and anionic dyes onto the activated carbon prepared from grapevine rhytidome. *Journal of Dispersion Science and Technology*, 33, 846-53, **2012**.
- [5] Hu E., Shang S., Tao X.-m., Jiang S., Chiu K.-l., Regeneration and reuse of highly polluting textile dyeing effluents through catalytic ozonation with carbon aerogel catalysts. *Journal of Cleaner Production*, 137, 1055-65, **2016**.
- [6] Song H., You J.-A., Chen C., Zhang H., Ji X.Z., Li C., Yang Y., Xu N., Huang J., Manganese functionalized mesoporous molecular sieves Ti-HMS as a Fenton-like catalyst for dyes wastewater purification by advanced oxidation processes. *Journal of Environmental Chemical Engineering*, **2016**.
- [7] Li H., Liu S., Zhao J., Feng N., Removal of reactive dyes from wastewater assisted with kaolin clay by magnesium hydroxide coagulation process. *Colloids and Surfaces A: Physicochemical and Engineering Aspects*, 494, 222-27, **2016**.
- [8] Sen S.K., Raut S., Bandyopadhyay P., Raut S., Fungal decolouration and degradation of azo dyes: A review. *Fungal Biology Reviews*, 30, 112-33, **2016**.
- [9] Han H., Wei W., Jiang Z., Lu J., Zhu J., Xie J., Removal of cationic dyes from aqueous solution by adsorption onto hydrophobic/hydrophilic silica aerogel. *Colloids and Surfaces A: Physicochemical and Engineering Aspects*, 509, 539-49, **2016**.
- [10] Zhigang Jia, Ziyu Li, Tao Ni, Li S., Adsorption of lowcost absorption materials based on biomass (*Cortaderia selloana* flower spikes) for dye removal: Kinetics, isotherms and thermodynamic studies. *Journal of Molecular Liquids*, **2016**.
- [11] Dotto G.L., Pinto L.A.d.A., Analysis of mass transfer kinetics in the biosorption of synthetic dyes onto *Spirulina platensis* nanoparticles. *Biochemical Engineering Journal*, 68, 85-90, **2012**.
- [12] Nabais J.V., Laginhas C., Carrott M.R., Carrott P., Amorós J.C., Gisbert A.N., Surface and porous characterisation of activated carbons made from a novel biomass precursor, the esparto grass. *Applied Surface Science*, 265, 919-24, **2013**.
- [13] Ofomaja A., Naidoo E., Modise S., Dynamic studies and pseudo-second order modeling of copper (II) biosorption onto pine cone powder. *Desalination*, 251, 112-22, **2010**.
- [14] Yang R., Liu G., Li M., Zhang J., Hao X., Preparation and N<sub>2</sub>, CO<sub>2</sub> and H<sub>2</sub> adsorption of super activated carbon derived from biomass source hemp (*Cannabis sativa* L.) stem. *Microporous and Mesoporous Materials*, 158, 108-16, **2012**.
- [15] Ozdemir I., Şahin M., Orhan R., Erdem M., Preparation and characterization of activated carbon from grape stalk by zinc chloride activation. *Fuel Processing Technology*, 125, 200-06, **2014**.
- [16] Djilani C., Zaghoudi R., Modarressi A., Rogalski M., Djazi F., Lallam A., Elimination of organic micropollutants by adsorption on activated carbon prepared from agricultural waste. *Chemical Engineering Journal*, 189, 203-12, **2012**.
- [17] Pezoti O., Cazetta A.L., Souza I.P., Bedin K.C., Martins A.C., Silva T.L., Almeida V.C., Adsorption studies of methylene blue onto ZnCl<sub>2</sub>-activated carbon produced from buriti shells (*Mauritia flexuosa* L.). *Journal of Industrial and Engineering Chemistry*, 20, 4401-07, **2014**.
- [18] Sathishkumar P., Arulkumar M., Palvannan T., Utilization of agro-industrial waste *Jatropha curcas* pods as an activated carbon for the adsorption of reactive dye Remazol Brilliant Blue R (RBBR). *Journal of Cleaner Production*, 22, 67-75, **2012**.
- [19] Saygılı H., Güzel F., Önal Y., Conversion of grape industrial processing waste to activated carbon sorbent and its performance in cationic and anionic dyes adsorption. *Journal of Cleaner Production*, 93, 84-93, **2015**.
- [20] Saygılı H., Güzel F., High surface area mesoporous activated carbon from tomato processing solid waste by zinc chloride activation: process optimization, characterization and dyes adsorption. *Journal of Cleaner Production*, 113, 995-1004, **2016**.
- [21] Anonymous, Hemp plant, agriculture statistics of Pakistan, in: b.o. statistics (Ed.), 28. 12. 2016.
- [22] Jawad A.H., Azharul M., Hameed B., Cross-linked chitosan thin film coated onto glass plate as an effective adsorbent for adsorption of reactive orange 16. *International Journal of Biological Macromolecules*, **2016**.
- [23] Hussain Gardazi S.M., Ashfaq Butt T., Rashid N., Pervez A., Mahmood Q., Maroof Shah M., Bilal M., Effective adsorption of cationic dye from aqueous solution using low-cost corncob in batch and column studies. *Desalin. Water Treat.*, 57, 28981-98, **2016**.
- [24] Haroon H., Ashfaq T., Gardazi S.M.H., Sherazi T.A., Ali M., Rashid N., Bilal M., Equilibrium kinetic and thermodynamic studies of Cr(VI) adsorption onto a novel adsorbent of *Eucalyptus camaldulensis* waste: Batch and column reactors. *Korean J. Chem. Eng.*, 33, 2898-907, **2016**.
- [25] Gardazi S.M.H., Rehman S., Ashfaq T., Ali M., Bilal M., Process Optimization of Hazardous Malachite Green (MG) Adsorption onto White Cedar Waste: Isotherms, Kinetics and Thermodynamic Studies. *Curr. Anal. Chem.*, Accepted, **2016**.
- [26] Kadirvelu K., Namasivayam C., Activated carbon from coconut coirpith as metal adsorbent: adsorption of Cd (II) from aqueous solution. *Advances in Environmental Research*, 7, 471-78, **2003**.
- [27] Zouboulis A.I., Lazaridis N.K., Matis K.A., Removal of toxic metal ions from aqueous systems by biosorptive flotation. *Journal of Chemical Technology and Biotechnology*, 77, 958-64, **2002**.
- [28] Elmoubarki R., Mahjoubi F., Tounsadi H., Moustadraf J., Abdennouri M., Zouhri A., El Albani A., Barka N., Adsorption of textile dyes on raw and decanted Moroccan clays: Kinetics, equilibrium and thermodynamics. *Water Resources and Industry*, 9, 16-29, **2015**.
- [29] Ai L., Li M., Li L., Adsorption of methylene blue from aqueous solution with activated carbon/cobalt ferrite/alginate composite beads: kinetics, isotherms, and thermodynamics. *Journal of Chemical & Engineering Data*, 56, 3475-83, **2011**.
- [30] Vaghetti J.C., Lima E.C., Royer B., Brasil J.L., da Cunha B.M., Simon N.M., Cardoso N.F., Noreña C.P.Z., Application of Brazilian-pine fruit coat as a biosorbent to removal of Cr (VI) from aqueous solution— Kinetics and equilibrium study. *Biochemical Engineering Journal*, 42, 67-76, **2008**.
- [31] Vasconcelos H.L., Guibal E., Laus R., Vitali L., Fávere V.T., Competitive adsorption of Cu (II) and Cd (II) ions on spray-dried chitosan loaded with Reactive Orange 16. *Materials Science and Engineering: C*, 29, 613-18, **2009**.
- [32] Zhang W., Zhang L.Y., Zhao X.J., Zhou Z., Citrus pectin derived porous carbons as a superior adsorbent toward removal of methylene blue. *Journal of Solid State Chemistry*, 243, 101-05, **2016**.
- [33] Zhang W., Zhang L.Y., Zhao X.J., Zhou Z., Citrus pectin derived ultrasmall Fe<sub>3</sub>O<sub>4</sub>@ C nanoparticles as a high-performance adsorbent toward removal of methylene blue. *Journal of Molecular Liquids*, 222, 995-1002, **2016**.

[34] Langmuir I., The adsorption of gases on plane surfaces of glass, mica and platinum. *Journal of the American Chemical society*, 40, 1361-403, **1918**.

[35] Freundlich U., Die adsorption in losungen. **1906**.

[36] Hutson N.D., Yang R.T., Theoretical basis for the Dubinin-Radushkevitch (DR) adsorption isotherm equation. *Adsorption*, 3, 189-95, **1997**.

[37] Dada A., Olalekan A., Olatunya A., Dada O., Langmuir, Freundlich, Temkin and Dubinin–Radushkevich isotherms studies of equilibrium sorption of Zn<sup>2+</sup> unto phosphoric acid modified rice husk. *Journal of Applied Chemistry*, 3, 38-45, **2012**.

[38] Zhou Q., Chen F., Wu W., Bu R., Li W., Yang F., Reactive orange 5 removal from aqueous solution using hydroxyl ammonium ionic liquids/layered double hydroxides intercalation composites. *Chemical Engineering Journal*, 285, 198-206, **2016**.

[39] Liu J., Wang X., Novel silica-based hybrid adsorbents: lead (II) adsorption isotherms. *The Scientific World Journal*, 2013, **2013**.

[40] Al-Degs Y.S., El-Barghouthi M.I., El-Sheikh A.H., Walker G.M., Effect of solution pH, ionic strength, and temperature on adsorption behavior of reactive dyes on activated carbon. *Dyes Pigments*, 77, 16-23, **2008**.

[41] Hajati S., Ghaedi M., Karimi F., Barazesh B., Sahraei R., Daneshfar A., Competitive adsorption of Direct Yellow 12 and Reactive Orange 12 on ZnS: Mn nanoparticles loaded on activated carbon as novel adsorbent. *J. Ind. Eng. Chem.*, 20, 564-71, **2014**.

[42] Kyzas G.Z., Deliyanni E.A., Lazaridis N.K., Magnetic modification of microporous carbon for dye adsorption. *J. Colloid Interf. Sci.*, 430, 166-73, **2014**.

© 2017 by the authors. This article is an open access article distributed under the terms and conditions of the Creative Commons Attribution license (<http://creativecommons.org/licenses/by/4.0/>).